Al-Nahrain Journal for Engineering Sciences **NJES** 28(3)481-492, 2025
http://doi.org/10.29194/NJES.28030481

The Seismic Response of a Shallow Foundation Supported on Geogrid-Reinforced Sand Soil

Ruqayah Al-khafaji[1], Qassun S. Mohammed Shafiqu[2*]

Authors affiliations:
1) Department of Civil Engineering, College of Engineering, Al-Nahrain University, Bagdad, Iraq
ruqayahhayder1@gmail.com

2*) Department of Civil Engineering, College of Engineering, Al-Nahrain University, Bagdad, Iraq
qassun.s.al-deen@nahrainuniv.edu.iq

Paper History:

Received: 21st Nov. 2024

Revised: 18th Feb. 2025

Accepted: 23rd Mar. 2025

Abstract

Shallow foundation suffers from considerable settlement, displacement and tilting under earthquakes. This is particularly due to the shaking associated with earthquakes that lead to the generation of horizontal seismic load transferred through the soil to the foundation. Also, liquefaction could take place during the earthquake in the saturated loose sand. To alleviate the detrimental effect of earthquakes, ground improvement is required. This study examines the response of the shallow square foundation rested on loose sand soil reinforced with geogrid reinforcement when subjected to 2023 Turkey earthquake by using a shaking table system. Different number of geogrid layers are installed; (one, two, three and four), also various geogrid configurations were examined which are (straight, trapezoidal and reverse trapezoidal). The acceleration response, settlement, horizontal displacement, rotation and pore water pressure developed in the sand soil and the shallow foundation during 2023 Turkey earthquake has been examined. The settlement and the horizontal displacement, foundation rotation, acceleration and pore water pressure were measured using rope displacement transducers, tilt sensors, accelerometers and pore water transducers respectively. The results showed that the acceleration amplifies when passing through loose sand. The results also indicated that the shallow foundation experienced noticeable settlement, horizontal displacement and rotation when subjected to the seismic loads. On the other hand, the installation of geogrid proved to be effective in controlling the problems associated with earthquakes. The optimum geogrid reinforcement is occurred when three layers of geogrid placed in reverse trapezoidal configuration (3RT) since it gave the best reduction in the acceleration amplification and the highest decrease in the foundation settlement, displacement and tilting which is about (60-66) %. Nevertheless, the effectiveness of geogrid minimizes when the sand soil becomes saturated. In addition, liquefaction occurs during earthquakes especially at the shallower depths because of the decrease in the shear strength of saturated soil.

Keywords: Geogrid Reinforcement, Foundation Rotation, Horizontal Displacement, Liquefaction, Sand Soil, Settlement, Shaking Table, Turkey Earthquake

الاستجابة الزلزالية للأساسات السطحية المدعومة بتربة رملية مسلحة بالمشبك الأرضي

رقيه حيدر كاظم، قاسيون سعد الدين

الخلاصة:

تعاني الأساسات الضحلة من هبوط، إزاحة، وميلان كبير تحت تأثير الزلازل. يعود ذلك بشكل رئيسي إلى الاهتزازات المرتبطة بالزلزال، التي تؤدي إلى توليد أحمال زلزالية أفقية تُنقل عبر التربة إلى الأساس. كذلك، في الرمال

الرخوة المشبعة بالمياه، قد يحدث التسييل أثناء الزلزال. للتخفيف من تأثيرات الزلازل الضارة، يُعد تحسين التربة ضروريًا. تهدف هذه الدراسة إلى فحص استجابة الأساسات الضحلة المربعة الموضوعة على التربة الرملية الرخوة والمعززة بالمشبك الأرضي عند تعرضها الى هزة تركيا ٢٠٢٣ باستخدام نظام طاولة الاهتزاز. تم تركيب عدد مختلف من طبقات المشبك الأرضي؛ (واحدة، اثنتان، ثلاث وأربع طبقات)، كما تم فحص تكوينات متنوعة للجيوجريد وهي: (مستقيمة، شبه منحرف، وشبه منحرف مقلوب). تم فحص استجابة التسارع، الهبوط، الإزاحة الأفقية، الدوران وضغط المياه المسامي المتولد في التربة الرملية المثبت عليها الأساس الضحل خلال زلزال تركيا ٢٠٢٣. تم قياس الهبوط والإزاحة الأفقية، دوران الأساس، التسارع وضغط المياه المسامي باستخدام مقاييس الإزاحة الحبلية، أجهزة استشعار الميلان، أجهزة قياس التسارع، وأجهزة قياس ضغط المياه المسامي على التوالي. أظهرت النتائج أن التسارع يتضخم عند مروره عبر التربة الرملية الرخوة. النتائج ايضا بينت تعرضت الأساسات السطحية لهبوط ملحوظ، وإزاحة أفقية، ودوران عند تعرضها للأحمال الزلزالية.على الطرف الأخر, المشبك الأرضي اثبت فعاليه في التحكم في المشاكل المرتبطة بالزلازل. وُجد أن التسليح الأمثل للمشبك الأرضي يحدث عند وضع ثلاث طبقات من المشبك الأرضي في تكوين شبه منحرف مقلوب (٣RT)، حيث حقق أفضل تقليل في تضخيم التسارع وأعلى انخفاض في هبوط الأساسات، والإزاحة، والميلان بنسبة تتراوح بين (٦٠-٦٦) %. ومع ذلك، فإن فعالية المشبك الأرضي تقل عندما تصبح التربة الرملية مشبعة بالمياه. بالإضافة إلى ذلك، يحدث التسييل أثناء الزلزال خاصةً في الأعماق الضحلة بسبب انخفاض قوة القص للتربة المشبعة بالمياه.

1. Introduction

When a shallow foundation is subjected to an earthquake, it suffers from an increase in settlement and tilting that could be detrimental to the building's safety and integrity. The shaking associated with earthquakes can result in many problems for shallow foundations involving undermining of footing bearing capacity under the effects of cyclic degradation of the strength under earthquake, footing failure under the sliding or overturning caused by the excessive amount of shear forces and bending moment associated with earthquake, soil liquefaction that lead to considerable settlement and titling of the foundation, and the softening of the loose sand when the pore water pressure redistributed after the earthquake. All these problems result in the inevitable failure of the foundation. This detrimental nature of earthquakes encourages researchers to find ways to minimize the impacts of earthquakes[1].

The response of shallow foundations can be enhanced by placing geosynthetic layers within the sand soil as soil reinforcement. The most common geosynthetic materials used as reinforcing elements in sand soil are geotextile, geocomposite and geogrid [2]. Geogrid is a plyometric material consisting of tensile ribs with apertures large enough to allow the interlock with the surrounding soil. The interlocking between the geogrid and the soil improves the shear strength of the soil [3]. Previous researches evaluating the bearing capacity of shallow foundations founded on soil reinforced with geosynthetics show the feasibility of using them as reinforcing materials. They all revealed the effectiveness of using geosynthetic materials as soil reinforcement since they increase the static bearing capacity of shallow foundations and decrease the settlement when incorporated within the optimal parameters. These parameters include the distance of the first geosynthetic (u/B), the distance between the successive layers (h/B), the width of the reinforcement layer (b/B), and the number of geogrid layers (N). The results showed that the optimal u/B, h/B, b/B and N are in the range of (0.25-0.5), (0.2-0.5), (2.5-5) and (2-5) layers respectively [2, 4-8] .The utilization of geosynthetic layer indicates the possibility of placing shallow foundation in unfavorable soil conditions. Thus, extensive studies have been carried out to comprehend how geosynthetic materials adjust foundation and soil behavior.

The uses of geosynthetics as soil reinforcement have been investigated by researchers such as [9] examined the liquefaction resistance of Solani sand reinforced with a geogrid sheet, natural coir and geosynthetic fibre. The tests were conducted on loose saturated sand with a relative density of 25% using a 1g shaking table system. The results showed that the liquefaction resistance increased by 31%, 91%, and 88% when five layers of geogrid, 0.75% coir fibre and 0.75% synthetic fibre were used respectively. The results also proved the effectiveness of reinforcement in decreasing the foundation settlement. This proposed modification method can be adopted in many applications such as roads, embankments, dams and mid-rise buildings. Dhanya et al., [10] indicated that the use of geogrid with geotechnical seismic isolation system (GSI) to support two-story building modelled by PLAXIS 2D that geogrid reinforced (GSI) is effective in reduce settlement, iner-story drift, tilting of the raft foundation and the superstructure. Xu et al., [11] investigated the performance of mid-rise buildings rested on geotextile-reinforced soil using the FLAC 3D program under two earthquake histories namely the 1994 Northridge Earthquake and 1999 Chichi Earthquake. The influence of stiffness, number of geotextile layers, vertical spacing between the layers and their length were examined in the parametric

NJES is an **open access Journal** with **ISSN 2521-9154** and **eISSN 2521-9162**

study. The results showed that the increase in the structural shear forces increased as the stiffness, the number of geotextile layers and length increased and decreased with the decrease in the vertical spacing between the layers due to the decrease in the energy dissipation induced by soil plasticity. The study also indicated that the geotextile layers placed near foundation edges withstand most of the stresses. In addition, the structure suffers from less permanent settlement, and rocking (foundation rotation in which one side of the foundation exposes tension and the other side is subjected to compression in the same magnitude) as the stiffness, length, and number of geotextile layers increase. This proved the significant influence of the geotextile arrangement on the seismic behaviour of mid-rise buildings. [12] examined the response of shallow foundation modelling 4 story building rested on saturated loose sand reinforced with geocomposite layers in different configurations under earthquake using a 1g shaking table system. The failure mechanism was appointed using a digital camera and a mesh of colored sand was utilized for analysis. The results indicated the settlement of a shallow foundation during a strong earthquake occurs in two phases. The settlement in the first phase is attributed to the soil movement in deeper depths underneath the footing. The settlement in the second phase involves the sinking of the foundation because of the decrease in the bearing capacity of the surface soil. It also found that reinforcing the sand soil can reduce pore water pressure at shallow depths with no alteration to the deformation shape, eliminate surface heave and increase soil resistance to liquefaction and hence delay and lower the foundation settlement.

Despite the previous research, there is limited research investigating the influence of geogrid reinforcement in different numbers and configurations on the performance of shallow foundations (spread footing) rested on loose sand under the effect of the 2023 Turkey.

2. Experimental set up

A 1g shaking table system locally- manufactured was used in this study. The shaking table consists of many mechanical parts, sensors, DAQ hardware and software. The mechanical parts of the shaking table are the frame, linear guard, shaft, table and ball screw and nuts as shown in Figure 1. The controlling and operating systems of the table consist of a servo driver, control box, software control and servo motor. This system is used for operating the shaking table and produces horizontal movement. The operation system is controlled by a laptop with a 2018 LabVIEW program that permits the insert of the earthquake data in the form of an Excel table for the time and displacement. The servo driver transmits the signal given by the program to the control box which transmits the signal to the servo motor and the servo motor then starts the movement. The servo motor is LCMT-7.5M02NB-180M48015B from LICHUAN Shenzhen Xinlichuan and the servo drive is fabricated by the same company. Figure 2 shows the components of the controlling and operating system of the shaking table.

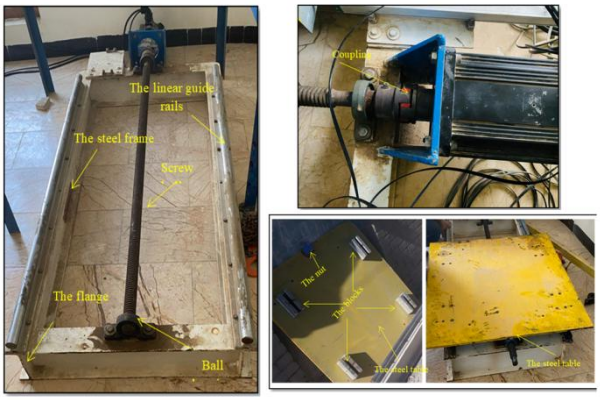

Figure (1): The mechanical parts of the shaking table

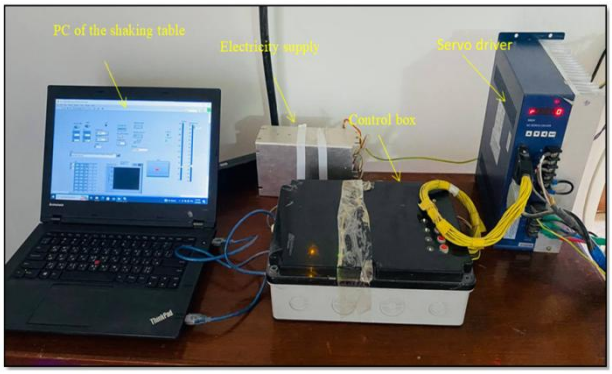

Figure (2): The controlling and operating system of the shaking table

A digital data acquisition system (DAQ) is used to collect the signals of the physical phenomena from the sensors and convert them into digital form utilizing software and computers. The DAQ parts involve DAQ hardware, DAQ software, sensors and signal conditioning.

The utilized sensors are displacement, acceleration, tilt sensors, and pore water pressure sensors. Four accelerometers were used, one located at the shaking for calibrating the acceleration and the other three are located at depths of 3, 6 and 12 cm from the top of the soil directly below the foundation. The accelerometers are ADXL335 type which is thin, small, light in weight, having low power and a good frequency response, linear, three-axis directions (x, y and z) with outputs required signal conditioning of voltages. Four displacement sensors were used; a linear variation displacement transducer with a maximum capacity of 500 mm, resistance of 5 kΩ ±20% and resolution of 0.05% was fixed on the shaking table to calibrate the horizontal displacement of the shaking table. The other three displacement sensors are rope displacement sensors (WFS-1000-P15-11R5) with 0,02A current and 24V from Fiaye utilized to examine the horizontal and vertical displacement of the square footing during shaking. One tilt sensor was utilized to measure the rotation of the foundation in both X and Y directions. It is GY25-A which is thin, and light in weight due to being manufactured from the thin quad flat package (TQFP), high accuracy, low power, dual-axis directions with signal-conditioned voltage outputs.

The pore water pressure of the saturated sand soil subjected to shaking was measured using two miniature pore pressure transducers with DMKY-1 type, one located at a depth of 3 cm and the other at a depth of 2 cm from the top of the soil directly underneath the foundation. This type of pore pressure transducer has a sensitivity of 1mV/V kPa, with an excitation voltage of 5 V, maximum capacity equal to 200 kN/m² and overload capacity of 120%. Figure 3 shows the utilized sensors.

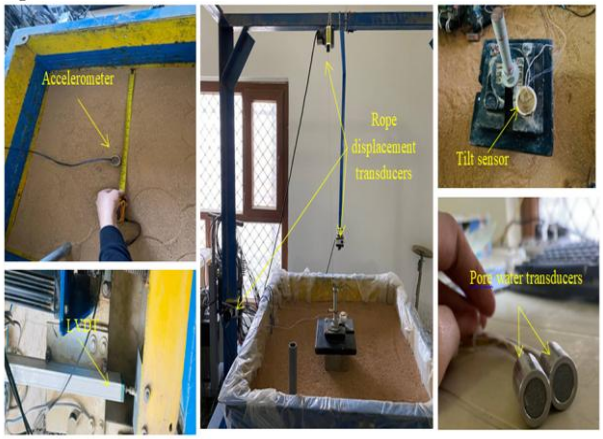

Figure (3): The sensors used in this research

Signal conditioning includes function such as signal attenuation, amplification and filtration to effectively acquire the signal of the sensor. In this study, the pore water transducer required signal conditioning to amplify the signal using amplifiers.

In this study, high-speed data transfer and acquisition (DAQ) from Nation Instruments NI PCI-6259 M series has been utilized (see Figure 4 a). Data Acquisition incorporates 32 analog inputs, 48 digital inputs, 1.25x106 samples per second, and 4 analog outputs. DAQ software indicates the LabVIEW computer software provided by National Instruments for the purpose of programming the signals supplied by the DAQ hardware (PCI-NI6259 card) see (Fig. 4.b). Laboratory Virtual Instrument Engineering Workbench (LabVIEW) is a programming language utilizing graphics and icons instead of lines and texts to produce applications. LabVIEW 2020 was programmed so that the readings of all the sensors can be displayed measured and saved on the computer during the tests. The data saved in the computer is analyzed by using another program called the DIAdem 2020 software program (see Figure 4 c). DIAdem is a software program that is used for management data processing, analysis and reporting.

A steel box with a dimension of (700 x 700) mm and a depth of 700 mm has been used. The container is fixed on the shaking table utilizing four steel plates having a U shape with four screws to restrain any movement. A steel frame with an L section with dimensions of (1.8 m x 1.10 m x 3 mm) has been used to attach the LVDT sensor. The water distribution network is placed inside the steel box to saturate the sand soil. It consists of perforated pipes with diameters of 0.75 inches arranged in square net pipes. Then, the square net pipes are covered with cloth to avoid the clogging of the holes. The gravel filter layer consisting of 4.75 mm (#4) and 2.36 mm (#8) was placed in the bottom of the container at a depth of 150 mm to work as a subbase for the sand soil and to avoid the drag of the soil with water during the drainage process. Figure 5 shows the steel container and the saturation system used in this study.

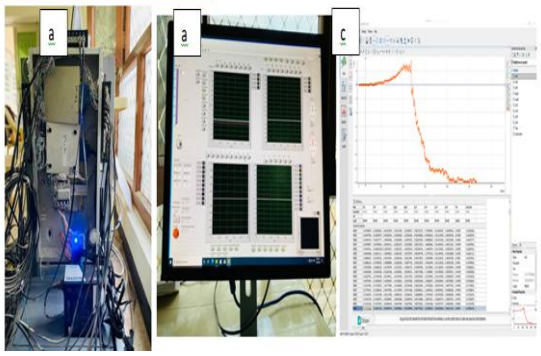

Figure (4): a) DAQ hardware b) LabVIEW program c) DIAdem program

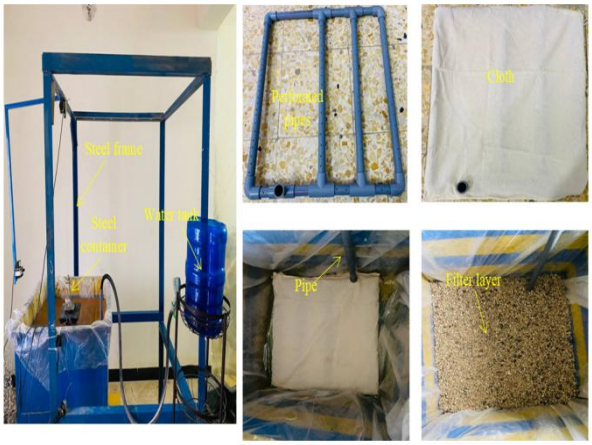

Figure (5): shows the container and the saturation system network

The earthquake adopted in this study is 2023 Turkey earthquake which has the details listed in Table 1. The earthquakes have been recorded by the Iraqi Metrological Organization and Seismology. Figure 6 shows the acceleration time history of the two historical earthquakes used in the study.

Table (1): details of 2023 Turkey earthquake

Region	date	Magnitude (Mw)	Modified Mercalli intensity (MMI)	Shake duration (Sec)	Maximum acceleration (g)	Seismic station code
Turkey	6/2/2023	7.8	XI	210	0.27	Kirkuk

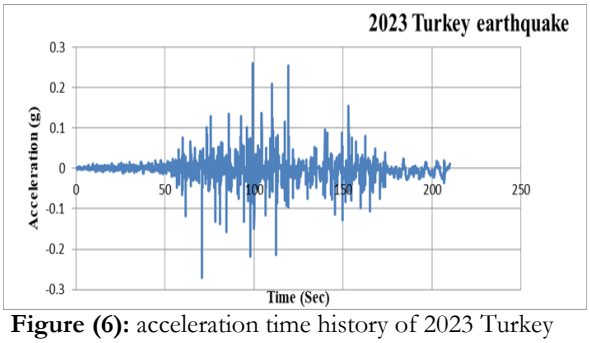

Figure (6): acceleration time history of 2023 Turkey earthquake

A spread footing made of aluminum block with square section (100 x 100x 60) mm was used that is equivalent to the prototype with dimensions of (1500 x 1500 x 900) mm since the adopted scale factor (λ = 15). The model footing weighs 2.5 kg and is made of aluminum as a solid block Figure 7a. The bearing capacity was calculated using the Hanson equation to determine the applied static load which was 6 kg.

The sand soil used in the study is the red sand known as "Al-Ekhether sand" collected from Karbala. It was prepared in the loose state with relative density of 30 % see Table 2. The soil was prepared in the dry and saturated state which is 100% saturated. The geogrid used in this study is InterAx NX750 geogrid. This geogrid is supplied by Tensar Company in the UK. The Tensar InterAx geogrid is manufactured from a coextruded, composite polymer sheet, which is then punched and oriented. The resulting structure consists of continuous and non-continuous ribs forming three aperture geometries (hexagon, trapezoid, and triangle) and an unimpeded suspended hexagon see Fig.7 b. The geogrid was placed within the soil at a depth of 0.3B for the first geogrid layer and the vertical distance between the layers in different configurations is shown in Table 3 and Figure 8.

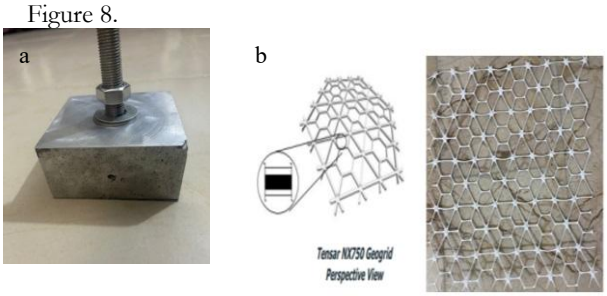

Figure (7): a) the spread footing b) the InterAx NX750 geogrid

Table (2): the soil properties

Soil properties	Relative density (%)	Maximum unit weight (kN/m³)	Minimum unit weight (kN/m³)	Unit weight (kN/m³)
value	30	17.87	14.91	15.69

Table (3): details of the geogrid configuration used in the study with their designation

Static weight (kg)	Geogrid configuration	cases in Figure 8	Designation
6	No geogrid	a	U
6	One geogrid layer	b	1G
6	Two straight geogrid layers	c	2G
6	Three straight geogrid layers	d	3G
6	Three geogrid layers in reversed trapezoidal configuration	e	3RT
6	Three geogrid layers in trapezoidal configuration	f	3T
6	Four geogrid layers in reversed trapezoidal configuration	g	4RT
6	Four geogrid layers in trapezoidal configuration	h	4T
6	Saturated no geogrid	i	S-U
6	Saturated with three reversed trapezoidal geogrid layers	k	S-3RT

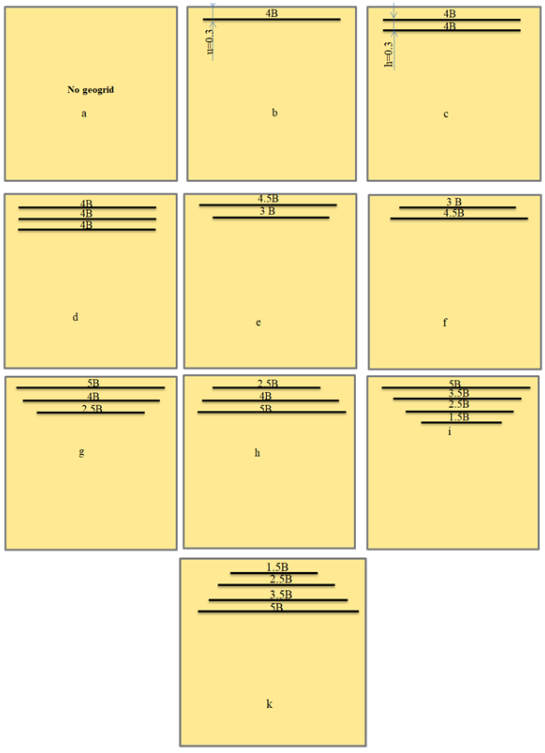

Figure (8): the different geogrid configurations used in the study.

3. The results and discussion

3.1 The acceleration results

During earthquakes, ground acceleration can be either amplified or reduced depending on many factors such as structure mass, and soil conditions including soil type, relative density, and saturation state. The acceleration amplification (AMF) which is a common expression used in wave propagation can be defined as the ratio of the peak ground acceleration at a specific point to the peak ground acceleration of the input acceleration (PGA point/PGA input acceleration).

The variations of the acceleration with time and at different depths of soil with and without geogrid reinforcement are given in Figure 9. The results show that the peak ground acceleration does not coincided at the different depths of soil. Also, it can be noticed that the ground acceleration amplified when passing through the loose sand and the amplification increase with depth and the maximum AMF was recorded at the points near the soil surface. This can be attributed to the presence of weak soil which is the loose sand that leads to amplification in acceleration. It is indicated that AMF occurs when the soil state is loose and as the densification of the

sand increase the AMF would be lowered. This is similar to the observations of [2, 13, 14].

The results also show that the geogrid can affect the soil response. The ground amplification is reduced as the geogrid is incorporated within the sand soil. As the number of geogrid increases from one to three, further reduction in amplification can be introduced. This may be attributed to the fact that geogrid in the soil increases the soil stiffness which means that the acceleration amplification would be lowered.

The alteration in geogrid reinforcement configuration also influences the soil performance. Placing three geogrid in reverse trapezoidal configuration (3RT) leads to a further decrease in the amplification particularly near the surface where the highest amplification occurred since the length of the geogrid in this area is increased. The lowest reduction in AMF is recorded in the case of the 4T configuration since the geogrid layers with the shortest lengths were placed at the depths close to the surface.

In the case of saturated loose sand, the results showed that the acceleration of the loose sand with and without geogrid reinforcement in the saturated state is considerably higher than that in the dry state. This can be attributed to the high total density of the saturated sand and the weakness of the saturated loose sand allowing further amplification in acceleration. The AMF of the saturated sand increases to 2.8 under the Turkey earthquake. The presence of the geogrid reinforcement in the optimum configuration has only a slight effect on the saturated sand behaviour due to the loss of contact between the geogrid and the sand soil in the saturated condition.

3.2 Settlement results

During an earthquake, the building foundation suffers from permanent settlement due to soil yielding. This can influence the entire performance of the structure and threaten the integrity of the foundation and in some cases; it leads to foundation collapse and building failure.

The vertical responses of the square foundation rested on soil with and without geogrid reinforcement are given in Figure 10. The results show that the settlement of the foundation increased with time as the earthquake intensity increased till reaching the maximum, after that it remained almost constant. Also, it was noticed that the highest settlement occurred when the soil incorporated no geogrid reinforcement with 7 mm.

The settlement of the foundation was reduced with the placement of geogrid reinforcement. As the number of geogrid increased, the settlement of the foundation reduced due to the increase in the stiffness of the sand soil in case of reinforcement. The lowest settlement was obtained when three geogrid layers reinforced the sand soil. The results showed that the settlement reduction ratio (the difference between the settlement without geogrid and with geogrid to the settlement without geogrid) was increased from 24% with one layer of geogrid to 40% with two layers and 60% with three layers.

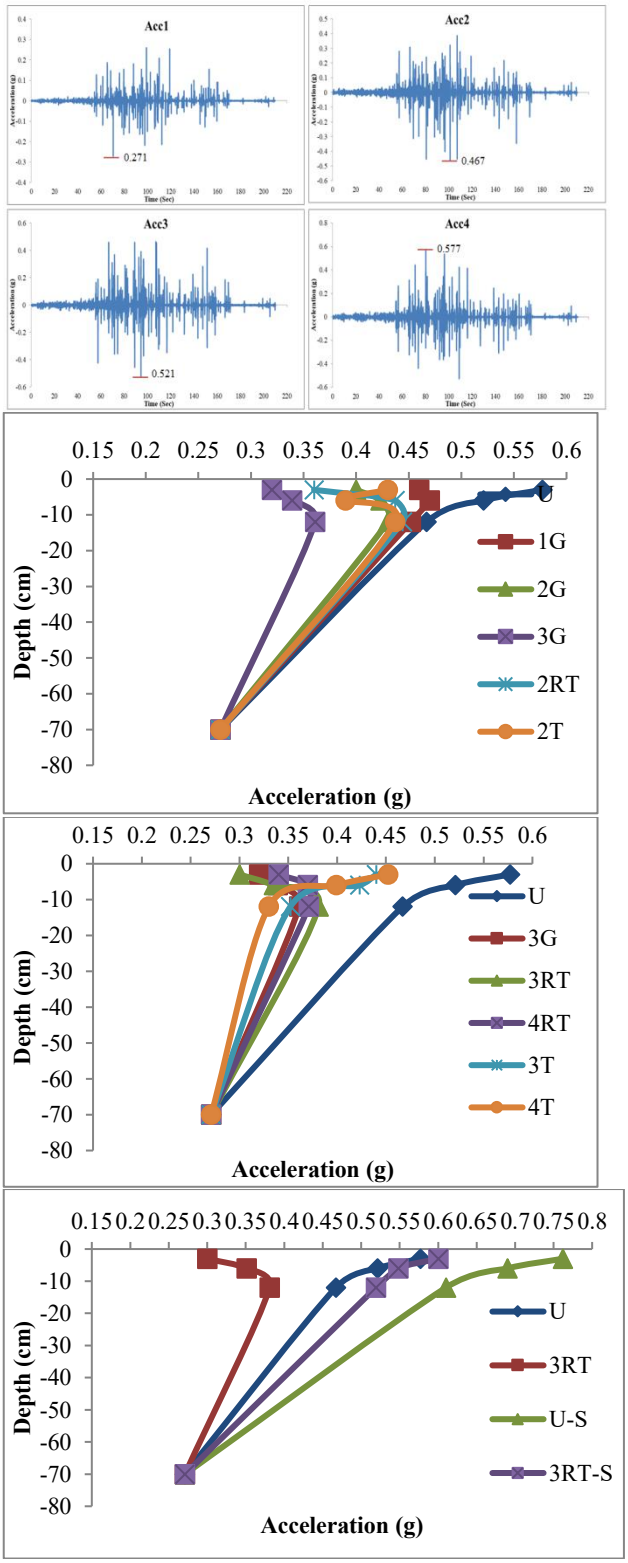

Figure (9): the variation of acceleration with time and depths during Turkey earthquake

The alteration in geogrid configurations gave different effects since the best performance was obtained in the case of 3RT configuration followed by 3G and then 4RT. This shows that although four geogrid layers were used in the case of 4RT, it would give an improvement of less than 3RT with the settlement reduction ratio reaching 70% due to the decrease in the length of the layers placed at the shallower depths. The lowest enhancement was given in the cases OF 4T and 3T since the lengthy layer

placed at the deeper depth where the inertial force resulted from soil structure interaction is the highest near the surface

In case of saturation, the settlement of the foundation on unreinforced sand increased considerably from 7 mm to 35 mm i.e. the settlement in the saturated state is about 5 times the settlement in the dry state. The geogrid effectiveness in the saturated sand is far less than that in dry sand with a settlement reduction ratio of 22% in the saturated loose sand. This is because the contact between the geogrid and the sand soil undermined significantly in the saturated soil under earthquake that may suffer from liquefaction.

3.3 Horizontal displacement results

When the foundation is subjected to an earthquake, vibration initiates at the interface between the soil and the foundation. The vibration gives rise to inertia forces in the forms of moment, torsion and base shear. These forces bring linear displacement and rotation in three directions X, Y and Z at the interface between the soil and the foundation. The horizontal response of the square foundation with and without geogrid reinforcement in X direction is given in and in Y direction is given in Figure 11 and Figure 12 respectively.

The results showed that the displacement in the X direction is higher than that in the Y direction since the earthquake intensity is the highest in the direction where the shaking is applied i.e. the X-axis. The result also showed that the horizontal displacement in X direction increased with time as the earthquake intensity increased and then decreased till settling at the end of the shaking. Meanwhile, in the latter direction, the displacement increased gradually till reaching the maximum and then settled.

The displacement reduction ratio (the difference between horizontal displacement without and with the horizontal displacement without geogrid) reaches (15-58) % as the number of geogrid increases from one to three layers in the case of loose sand. [11] indicated that the maximum lateral deflection decreased as the number of geosynthetic layers increased since the plastic deformation caused by soil yielding could be restrained more efficiently, hence the foundation would experience less permeant deformation. Also, the geogrid reinforcement would exert a confinement effect that developed between the soil and the geogrid layers, in addition to the mobilized tensile forces resisting the seismic forces. Thus, the maximum lateral displacement of the foundation decreased.

The variation in the lengths of geogrid layers is also an influential factor in the performance of the square foundation. In both two and three reverse trapezoidal configurations, the horizontal displacement in both the X and Y axes are better than that of the straight length, while the 2T 3T and 4T gave improvement less than 2G and 3G. The horizontal displacement reduction ratio of 3RT was 66% in the X-axis, and 62% in the Y-axis. It is true since the intensity of the base shear and moment are concentrated at the interface between the soil and the foundation. Hence, the stiffer this layer, the better the performance of the foundation can be gained.

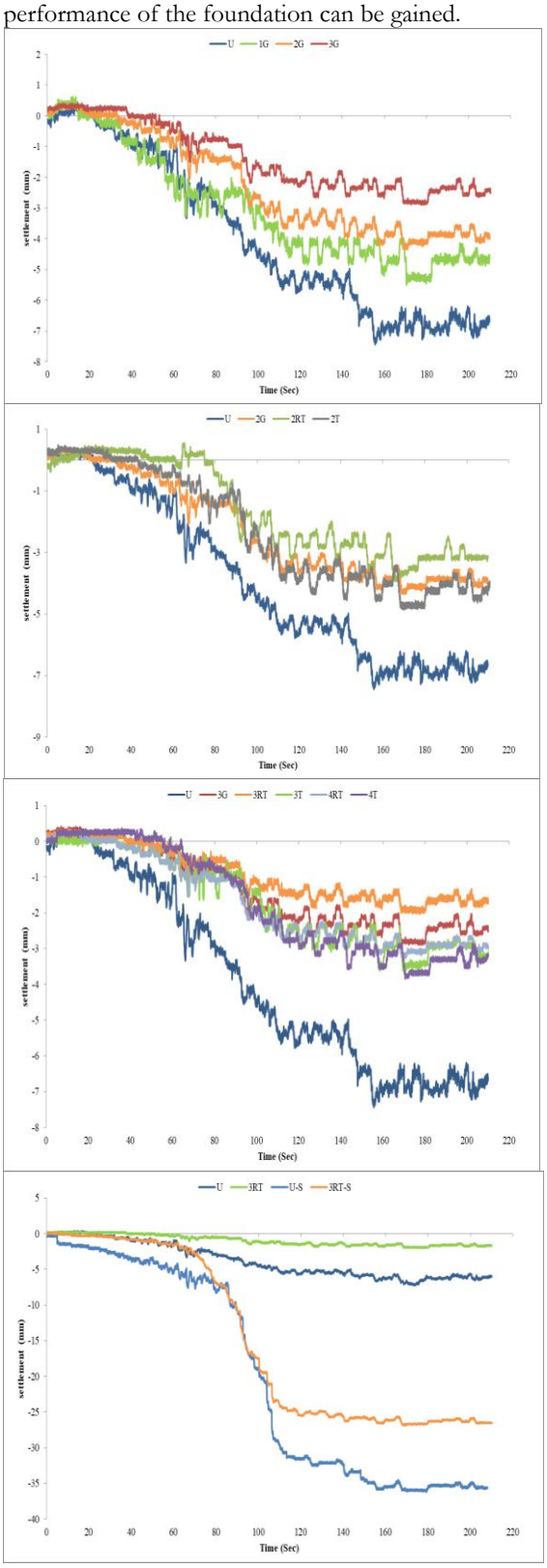

Figure (10): the settlement of square foundation rested on soil with and without geogrid reinforcement under Turkey earthquake

The saturation is indicated to be a critical case in earthquakes since the loose sand soil is susceptible to liquefaction due to the decrease in the contact between the particles which leads to a consequence decrease in the shear strength leaving the soil suffering considerable later deformation. In this

study, the horizontal displacement in X and Y of saturated unreinforced sand increased by 2.1 times (from 27 mm to 57 mm) and 1.9 times (from 14 mm to 26.8 mm) respectively. The effectiveness of geogrid in reinforcing the soil is lowered due to the high excess pore water pressure and the low shear strength so the confinement effect and interlocking effect of the geogrid and the soil is sustainably decreased.

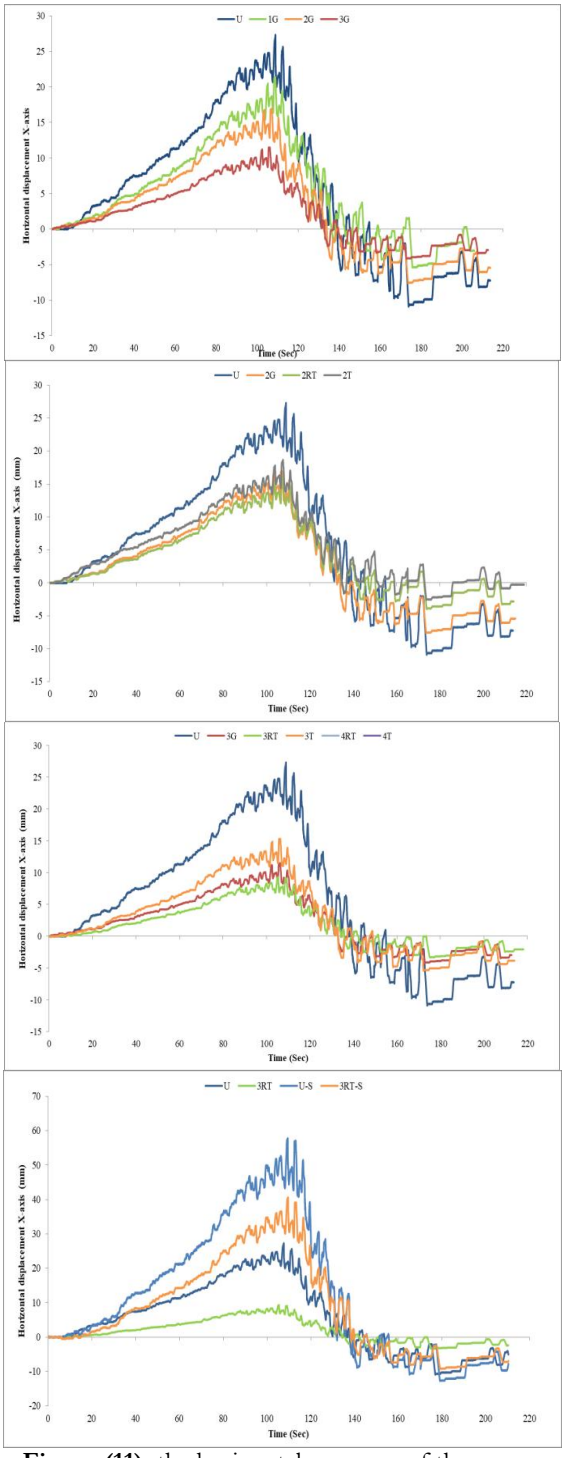

Figure (11): the horizontal response of the square foundation rested on soil with and without geogrid under Turkey earthquake- X direction

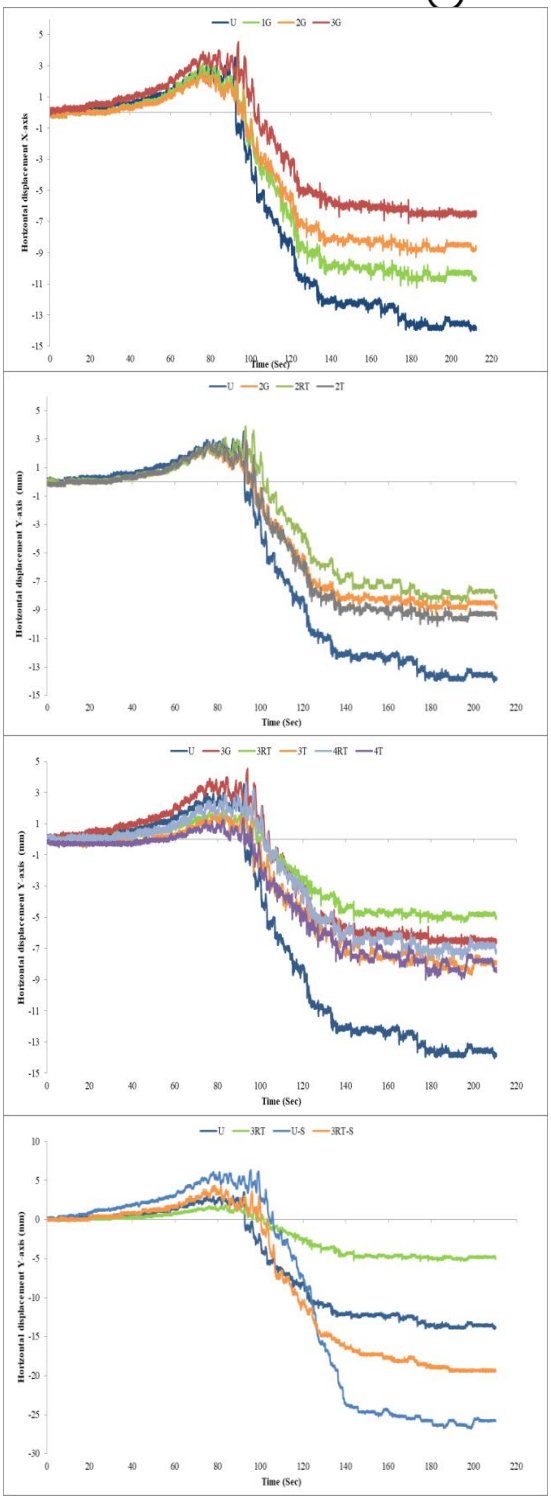

Figure (12): the horizontal response of the square foundation rested on soil with and without geogrid under Turkey earthquake- Y direction

3.4 Tilting result

When the soil underneath the foundation vibrates during the earthquake, the foundation can experience tilting in both X and Y directions because of the differential settlement produced due to soil yielding. The results of rotation in the X and Y axes are given in Figure 13 and Figure 14 respectively.

The result showed that the foundation tilting in both X and Y directions are comparable with each other, nevertheless, each of them rotates differently. In the X direction, the foundation rotation is in the

positive X-axis while in the Y-direction, the rotation is about the negative Y-axis. In the case of U soil, the tilting of the foundation was 4.240 in the X direction, and it was 3.30 in the Y direction.

The geogrid reinforcement decreases the foundation's permanent rotation in X and Y reactions. The improvement increases as the number of geogrid increases and as with the placement of the length layers near the surface. The optimum performance was given in the case of 3RT, followed by 3G and 4RT noticing that 3RT is better than 4RT since the length of the second layer was less than that in the case of 3RT. The lowest enhancement percentage was given with 4T, 3T, 1G, and 2G since the 4T and 3T have geogrid with short lengths close to the surface; hence the improvement level was only 36% and 40% in the X-axis. Meanwhile, the 1G and 2G gave improvement by 19% and 33% since no sufficient stiffness can be offered by decreasing the number of geogrid layers.

The saturation results in the sinking of the foundation in the loose sand causing permeant settlement and tilting. The foundation rotation in U soil was 10.710 and 7.420 in the X and Y directions respectively. The placement of the optimum geogrid configuration (3RT) gave less improvement ratio (the rotation reduction ratio decreased from 63% to 44% in the X direction and from 60% to 25% in the Y-axis as the soil state changed from dry to saturate).

3.4 Pore Water Pressure

The variation of pore water pressure has been examined using two pore water transducers placed directly underneath the foundation at depths 3 cm and 12 cm representing PWP1 and PWP2 respectively. The results of pore water pressure under Turkey earthquake in both unreinforced sand and sand with 3RT configuration are given in Figure 15.

The results showed that the pore water pressure increases with time till reaching the maximum value after that it returns to its initial value. This indicates the fact that during the earthquake, loose saturated sand experiences a decrease in the shear strength and an increase in the excess pore water pressure during the earthquake.

The liquefaction ratio (ru) = (Δu / σ') represents the ratio of the excess pore water pressure (Δu) to the effective strength of the soil ($\sigma'=\gamma h$). The liquefaction takes place when ru is equal to or more than a unity. Table 4 shows the liquefaction potential of the sand soil with and without reinforcement. From the table, it can be noticed that the pore water pressure developed at a depth of 12 cm is higher than that at a depth of 3 cm. Nevertheless, the liquefaction occurred at a depth of 3 cm due to the low soil column above it resulting in low effective overburden pressure. The liquefaction occurred in the sand with and without reinforcement. Although the liquefaction ratio decreased with geogrid, it was not adequate to prevent the liquefaction. The improvement is attributed to the fact that geogrid acts as a semi-permeable layer lowering the potential ratio during the earthquake.

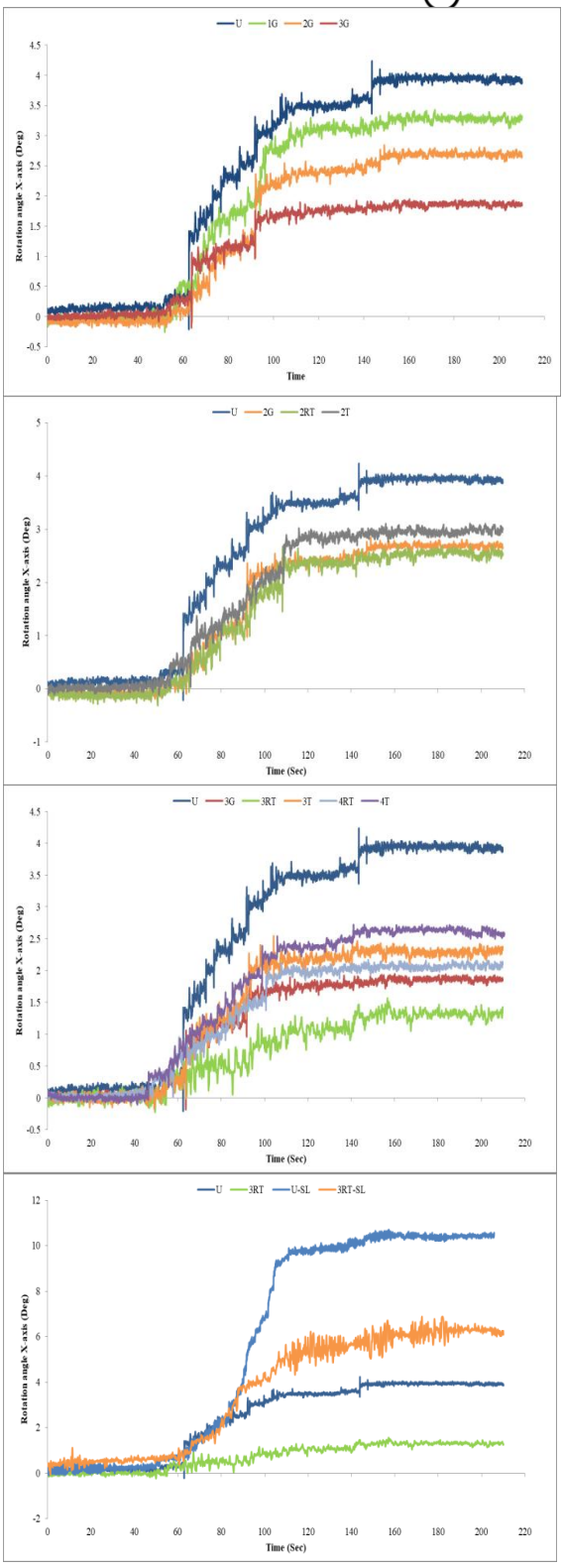

Figure (13): tilting of the square foundation rested on soil with and without geogrid under Turkey earthquake- X direction

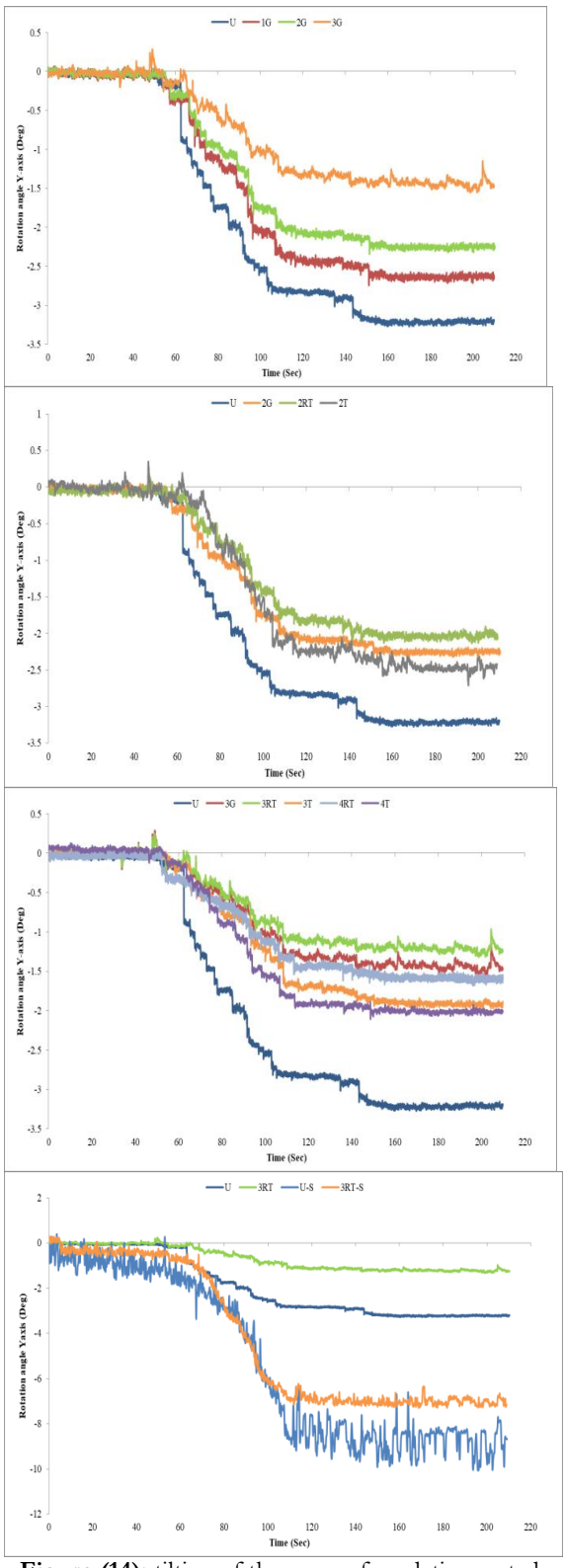

Figure (14): tilting of the square foundation rested on soil with and without geogrid under Turkey earthquake- Y direction

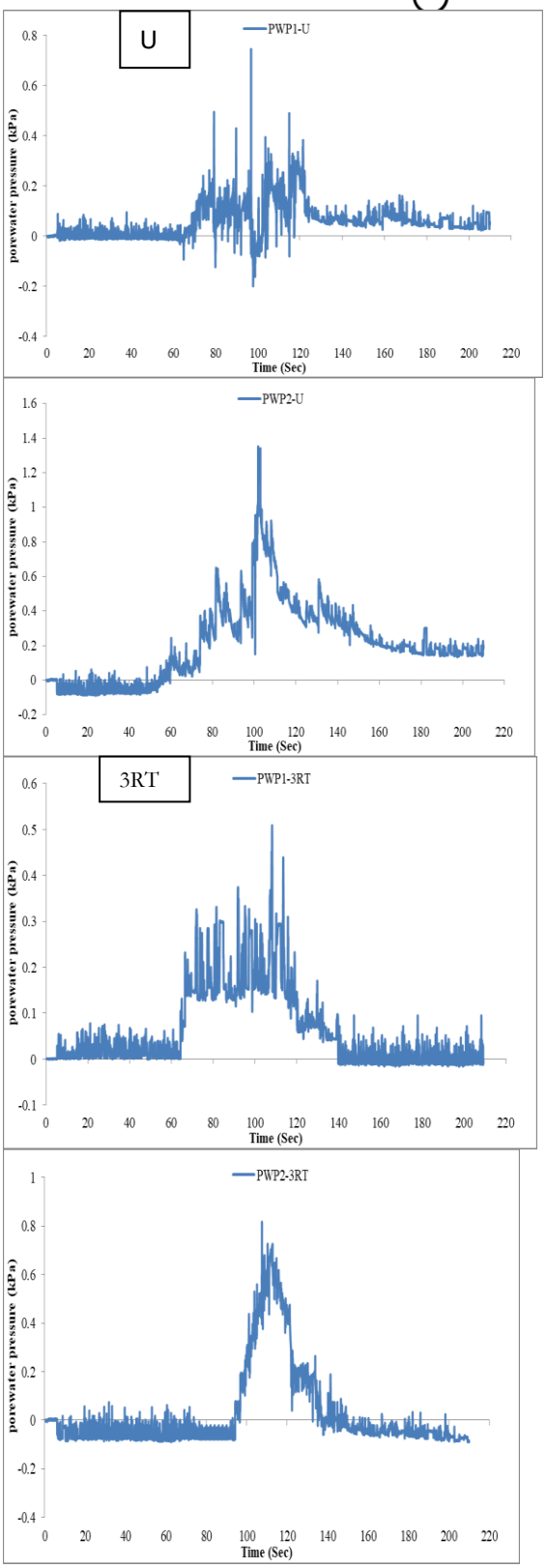

Figure (15): pore water pressure developed in the soil a) without reinforcement (U) b) with 3RT reinforcement

Table (4): the liquefaction ratio of the saturate loose sand with and without geogrid reinforcement

Shaking history	Soil condition	PWP	Max PWP	σ′	R_u	state
Turkey	U	PWP1	0.75	0.47	1.6	liquefied
		PWP2	1.35	1.88	0.72	Non-liquefied
	3RT	PWP1	0.53	0.47	1.34	liquefied

		PWP1	0.82	1.88	0.44	Non-liquefied

4. Conclusion

The response of the shallow square foundation rested on geogrid-reinforced sand soil subjected to the 2023 Turkey earthquake was examined using a shaking table. From this study, the following can be concluded:

- When the earthquake passes through the loose sand soil, the acceleration amplifies consequently. The maximum AMF occurred near the surface. The reinforcement of the sand with geogrid would lower the AMF. The amplification of acceleration increases as the soil becomes saturated. The best reduction in amplification was occurred with 3RT due to the placement of the lengthy layers near the soil surface.
- The settlement and the horizontal displacement of the square foundation increase due to the earthquake. Further increase in the foundation displacement in all directions is noticed when the sand soil is saturated.
- The horizontal displacement of the foundation in the X direction is higher than that in the Y direction since the intensity of the earthquake is the highest in the direction of application that is the X direction.
- The placement of geogrid decreases the foundation displacement in the horizontal and vertical directions. The vertical and horizontal response of the footing decreases as the number of geogrid layers increases. The alterations in geogrid configuration to 3RT, 3G, and 4RT resulted in further improvement in the performance of the shallow foundation. The 3T and 4T configuration gives the lowest improvement among all the configurations.
- The tilting of the foundation in X and Y directions is relatively comparable. The tilting of the foundation reduces with the increase in the number of geogrid layers and the application of different geogrid configurations.
- The geogrid proved to be effective in improving the soil response during earthquakes because geogrid acted as a stiff layer increasing the shear strength and stiffness of the soil. The geogrid provides membrane effect, confinement effect and interlocking effect that are responsible for the optimized performance.
- The use of geogrid in saturated loose sand gives improvement in deformation, and rotation less than in the case of dry sand. This can be attributed to the fact that the contact between the soil particles decreases significantly in the case of saturation hence the interlocking between the soil and the geogrid is undermined.
- During the earthquake, the saturated loose sand suffers from an increase in the excess pore water pressure to the limit exceeding the effective overburden pressure. This leads to soil liquefaction, particularly near the soil surface where the soil column is very low.

9. References:

[1] V. K. Puri and S. Prakash, "Shallow foundations for seismic loads: Design considerations," in Proc. 7th Int. Conf. Case Histories Geotech. Eng., Chicago, IL, May 3, 2013. https://scholarsmine.mst.edu/icchge/7icchge/session14/6

[2] J.-Q. Wang, et al., "Influence of reinforcement-arrangements on dynamic response of geogrid-reinforced foundation under repeated loading," Constr. Build. Mater., vol. 274, p. 122093, 2021. DOI:10.1016/j.conbuildmat.2020.122093

[3] M. Ziegler, "Application of geogrid reinforced constructions: History, recent and future developments," Procedia Eng., vol. 172, pp. 42-51, 2017. DOI:10.1016/j.proeng.2017.02.008

[4] Z. Zhang, et al., "Influence of number of geosynthetic layers on the performance of geosynthetic-reinforced pile-supported earth platforms on soft soil: Numerical study," in Proc. Int. Conf. Transp. Infrastruct. Mater., Qingdao, China, 2017. DOI:10.12783/dtmse/ictim2017/10045

[5] A. Morsy, et al., "A new generation of soil-geosynthetic interaction experimentation," Geotext. Geomembr., vol. 47, no. 4, pp. 459-476, 2019. DOI:10.1016/j.geotexmem.2019.04.002

[6] A. M. Morsy and J. G. Zornberg, "Soil-reinforcement interaction: Stress regime evolution in geosynthetic-reinforced soils," Geotext. Geomembr., vol. 49, no. 1, pp. 323-342, 2021. DOI:10.1016/j.geotexmem.2020.10.004

[7] R. J. Bathurst and F. M. Naftchali, "Geosynthetic reinforcement stiffness for analytical and numerical modelling of reinforced soil structures," Geotext. Geomembr., vol. 49, no. 4, pp. 921-940, 2021. DOI:10.1016/j.geotexmem.2021.01.003

[8] A. C. Pires and E. M. Palmeira, "The influence of geosynthetic reinforcement on the mechanical behaviour of soil-pipe systems," Geotext. Geomembr., vol. 49, no. 5, pp. 1117-1128, 2021. DOI:10.1016/j.geotexmem.2021.07.005

[9] B. K. Maheshwari, H. Singh, and S. Saran, "Effects of reinforcement on liquefaction resistance of Solani sand," J. Geotech. Geoenviron. Eng., vol. 138, no. 7, pp. 831-840, 2012. DOI:10.1061/(ASCE)GT.1943-5606.0000646

[10] J. Dhanya, A. Boominathan, and S. Banerjee, "Response of low-rise building with geotechnical seismic isolation system," Soil Dyn. Earthq. Eng., vol. 136, p. 106187, 2020. DOI:10.1016/j.soildyn.2020.106187

[11] R. Xu and B. Fatahi, "Influence of geotextile arrangement on seismic performance of mid-rise buildings subjected to MCE shaking," Geotext. Geomembr., vol. 46, no. 4, pp. 511-528, 2018. DOI:10.1016/j.geotexmem.2018.03.007

[12] H. Bahadori, et al., "Shaking table tests on shallow foundations over geocomposite and geogrid-reinforced liquefiable soils," Soil Dyn. Earthq. Eng., vol. 128, p. 105896, 2020. DOI:10.1016/j.soildyn.2019.105896

[13] N. Srilatha, G. M. Latha, and C. Puttappa, "Seismic response of soil slopes in shaking table tests: Effect of type and quantity of reinforcement," Int. J. Geosynth. Ground Eng., vol. 2, p. 1-13, 2016. DOI:10.1007/s40891-016-0074-2

[14] H. J. Park, et al., "Investigation of the dynamic behaviour of a storage tank with different foundation types focusing on the soil-foundation-structure interactions using centrifuge model tests," Earthq. Eng. Struct. Dyn., vol. 46, no. 14, pp. 2301-2316, 2017. DOI:10.1002/eqe.2905